Available online at www.sciencedirect.com
SCIENCE DIRECT
Journal of Sound and Vibration 296 (2006) 1028–1038
JOURNAL OF SOUND AND VIBRATION
www.elsevier.com/locate/jsvi

Short Communication

Damage detection in rods by means of the wavelet analysis of vibrations: Influence of the mode order

E. Castro[a], M.T. García-Hernandez[a], A. Gallego[b,*]

[a]Dpto. de Física, Escuela Politécnica Superior, Universidad de Jaén, 23071 Jaen, Spain
[b]Dpto. de Física Aplicada, E.U. Arquitectura Técnica, Universidad de Granada, 18071 Granada, Spain

Received 21 January 2005; received in revised form 29 December 2005; accepted 6 February 2006
Available online 12 June 2006

Abstract

This communication deals with the detection of damage in rods using free axial vibrations. A density and a stiffness reduction were considered as local defects. The displacement along the damaged rod at a fixed time was the signal used to assess the presence and location of defects through wavelet transform. A study of the influence of the mode order on damage detection is presented. We demonstrate that detection quality for a particular mode depends on the combination of two factors: the order of the mode and the location of the defect. As for the first factor, the higher the order of mode, the better the detection for both kinds of defects. The second factor depends on the kind of defect; if it affects density, its closeness to an antinode of displacement favors its detection. However, if it affects stiffness, the closeness to a node of displacement (antinode of the stress) improves its detection.

1. Introduction

In this communication, we propose to solve numerically the wave equation of longitudinal vibrations propagating in rods where a local reduction of density or stiffness has been introduced [1]. The aim of this inhomogeneity is to simulate local damage (crack, corrosion, etc.). The subsequent implementation of the corresponding detection leads to an algorithm that allows us to assess the structural health of the rod. Defects, in general almost unavoidable, result in a decrease in mass, stiffness, strength and safety of structural elements, for which reason their detection and locatization is very important. In the past few years, many researchers have exhibited interested in this subject, which now constitutes an autonomous research field known as "structural health monitoring" (SHM) [2].

There are various SHM levels of damage identification in a structure: Level 1: damage detection; Level 2: damage location; Level 3: quantification of the degree of damage; Level 4: estimation of the remaining service life. The most usual SHM techniques are ultrasonic methods [3] and vibration-based methods [4]. The vibration methods are based on the occurrence that damage in a structure produces a local increase in flexibility which induces changes in the dynamic properties of the structure. The analysis of these changes can

*Corresponding author. Tel.: +34 958249508; fax: +34 958243104.
E-mail address: antolino@ugr.es (A. Gallego).

0022-460X/$ - see front matter © 2006 Elsevier Ltd. All rights reserved.
doi:10.1016/j.jsv.2006.02.026

be used for damage identification. In recent years, the wavelet transform (WT) has been proposed as a promising mathematical tool for damage detection and localization, in light of its ability to locally analyze a signal. Liew and Wang applied the WT to spatial problems, specifically to identify cracks in structures [5]: using free vibrations of cracked beams with a local reduction of stiffness, they showed that the wavelet coefficients calculated along the beam presented a maximum precisely at the crack location. Further papers dealing with beams, plates or frame structures have validated this technique as a promising research tool [5–15]. The majority of these papers deal with the use of the spatial wavelet applied to free vibrations, however; to date, no study of the quality of damage detection versus the order of vibration mode has been presented. The main objective of our contribution is to present the results of this study for the two main kinds of defects: alterations in density and stiffness. In both cases, the vibrational response of the rod was obtained numerically by means of the network simulation method (NSM) as explained in Ref. [16]. Similar results are obtained via the finite elements method (FEM) [17].

2. The physical model and its numerical solution

The wave equation for axial vibrations in a homogeneous thin rod of length l is given by [18]

$$\frac{\partial^2 \xi}{\partial x^2} = \frac{1}{c^2}\frac{\partial^2 \xi}{\partial t^2}, \tag{1}$$

where ξ is the longitudinal displacement, c is the phase velocity and x and t are the position in the rod and the time, respectively. The stress, $\sigma(x,t)$, is given by

$$\sigma = -Y\frac{\partial \xi}{\partial x} \tag{2}$$

with $c = (Y/\rho)^{1/2}$, ρ and Y being the density and the Young modulus of the material, respectively. The wave equation, with boundary conditions at $x = 0$ and l, has been numerically solved with the NSM by dividing the rod into N cells of equal length Δx (see Refs. [16,17] for details). In particular, a fixed–fixed rod was considered: $\xi(l, t) = 0$ and $\xi(0, t) = 0$.

In this paper a damaged rod—i.e., a rod with a local defect—is the case in point. Physically, the defect can be represented as a change in mechanical properties such as density and/or stiffness that affects the damaged region. We considered the smallest possible extension of the damaged region: affecting only a single cell, Δx. This defect representation illustrates damage of a real part in an approximate manner, but the simplification is deemed accurate in light of the hypothesis of the numerical study. The modelling of this local defect in the rod can be carried out by modifying the parameters of the cell at which the defect is located. We will consider n_d to be the order of this cell. Thus, the position of the defect is given by $x_d = n_d\Delta x$. The intensity of the defect can be quantified by the relationship between ρ and ρ_d for a density defect, where ρ_d is the modified density of the rod where the defect is located; and between Y and Y_d for a stiffness defect, where Y_d is the modified Young modulus of the rod where the defect is located. For this reason, we define the intensity of a density defect as

$$\mathrm{Id}(\%) = 100\,\frac{\rho - \rho_d}{\rho} \tag{3}$$

and the intensity of a stiffness defect as

$$\mathrm{Is}(\%) = 100\,\frac{Y - Y_d}{Y}. \tag{4}$$

For an undamaged rod, the nth mode shape for longitudinal vibrations is theoretically well known [18]:

$$\psi_n^u(x) = \sin(\beta_n x), \quad \beta_n = n\,\frac{\pi}{L}. \tag{5}$$

If the rod has a defect (of type density or stiffness) located at x_d, along a fraction of 1/150 of the length of the rod, it is not possible to obtain the mode shapes theoretically, and so they must be derived either numerically or experimentally. Yet we can elaborate a numerical model for longitudinal vibrations, where the defect at x_d can be incorporated in the way explained earlier. Given this model of the damaged rod, it is

possible to introduce as the initial condition the nth mode of the undamaged rod, i.e. $\xi_n^d(x,0) = \psi_n^u(x)$, where $\psi_n^u(x)$ is given by Eq. (5). By numerically solving the model with this initial condition, the vibration of the damaged rod can be obtained for all times and positions.

3. Numerical results: damage detection

It can be easily demonstrated that no apparent difference exists between the response of the damaged, $\xi_n^d(x)$, and undamaged, $\xi_n^u(x)$, rods. The reason is basically that the extension and the intensity of the defects are too small to evidently affect the low-order (low frequency) natural vibrations. However, the defects can be detected and located by means of the WT. Let $W_n^d(x,j)$ and $W_n^u(x,j)$, respectively, denote the continuous wavelet transform (CWT) of signals $\xi_n^d(x)$ and $\xi_n^u(x)$, which are a function of the position x along the rod and the scale j. Although, as shown in Ref. [6], detection of the defect is equally possible using either CWT or discrete wavelet transform (DWT), in this case we opted for CWT, following the methodology of Douka [10], in order to present a brief comparative study to illustrate how the results change depending on the scale chosen (the scale is considered to be continuous in the CWT and discrete in the DWT). Moreover, the CWT algorithms generally provide for greater accuracy.

Fig. 1 shows the absolute value of $W_1^d(x,2)$ obtained using the Symmlet 4 as mother function (the more commonly used in the bibliography) for a rod with a density and stiffness defect, both at $x_d = 0.4767$ m, with $\mathrm{Id} = \mathrm{Is} = 0.1\%$. In both cases a big peak is clearly seen just where the defect is located. Likewise, two additional large peaks appear at the positions where the boundary conditions are applied ($x = 0$ and 1 m), suggesting as a misleading result the presence of non-existent defects. This problem can be overcome by using the difference between the WTs for damaged and undamaged samples as a detection function, i.e.:

$$\mathrm{WC}_n(x,j) = W_n^d(x,j) - W_n^u(x,j). \tag{6}$$

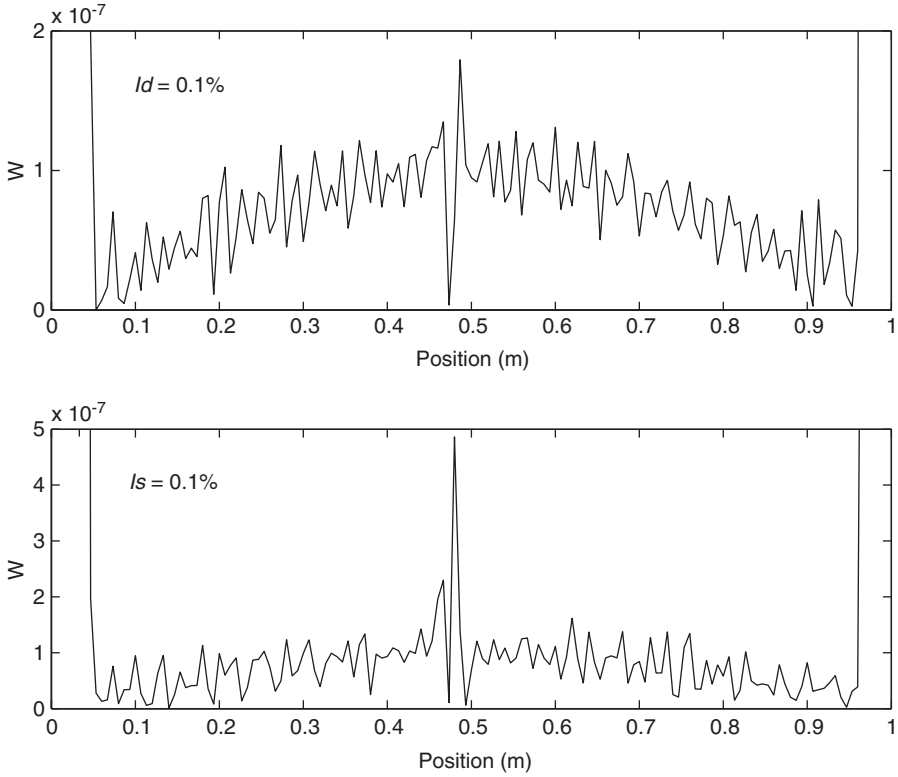

Fig. 1. Upper: $W_1^d(x,2)$ with $\mathrm{Id} = 0.1\%$; lower: $W_1^d(x,2)$ with $\mathrm{Is} = 0.1\%$. Symmlet-4 wavelet. Defect at $x_d = 0.4767$ m.

Figs. 2 and 3 show the absolute value of WC_1 for scales from $j = 1$ to 20, for density and stiffness defects, respectively, with Id = Is = 0.1%. The fact that no peaks appeared at $x = 0$ and 1 m, shows the utility of the WC in avoiding the boundary effect. It is also seen that for the majority of the scale values, a peak is present at $x_d = 0.4767$ m, thus indicating a very good level of defect detection.

Taking into account the physical sense of scales, we can suppose that smaller scales correspond to a more suitable localization and detection, considering that we are looking for singularities. It can be observed in Figs. 2 and 3 that the peak width increases according to scale, worsening the localization. Yet the amplitude of the peak also increases at the beginning, when j increases, then reaches a maximum near $j = 9$ and then decreases. Obviously, when the amplitude is higher, detection is enhanced. Stiffness-type defects are detectable and localizable at all scales, while density-type defects are not detectable at scales $j = 1$, 18, 19 and 20. Summarizing: (1) at lower scales the precision of localization improves because the peak width becomes lower. (2) Highest peak amplitudes are reached at intermediate scales. (3) If the scale is too high or too low, it is possible that an optimal detection degree will not be achieved, especially for density type defects of low intensity.

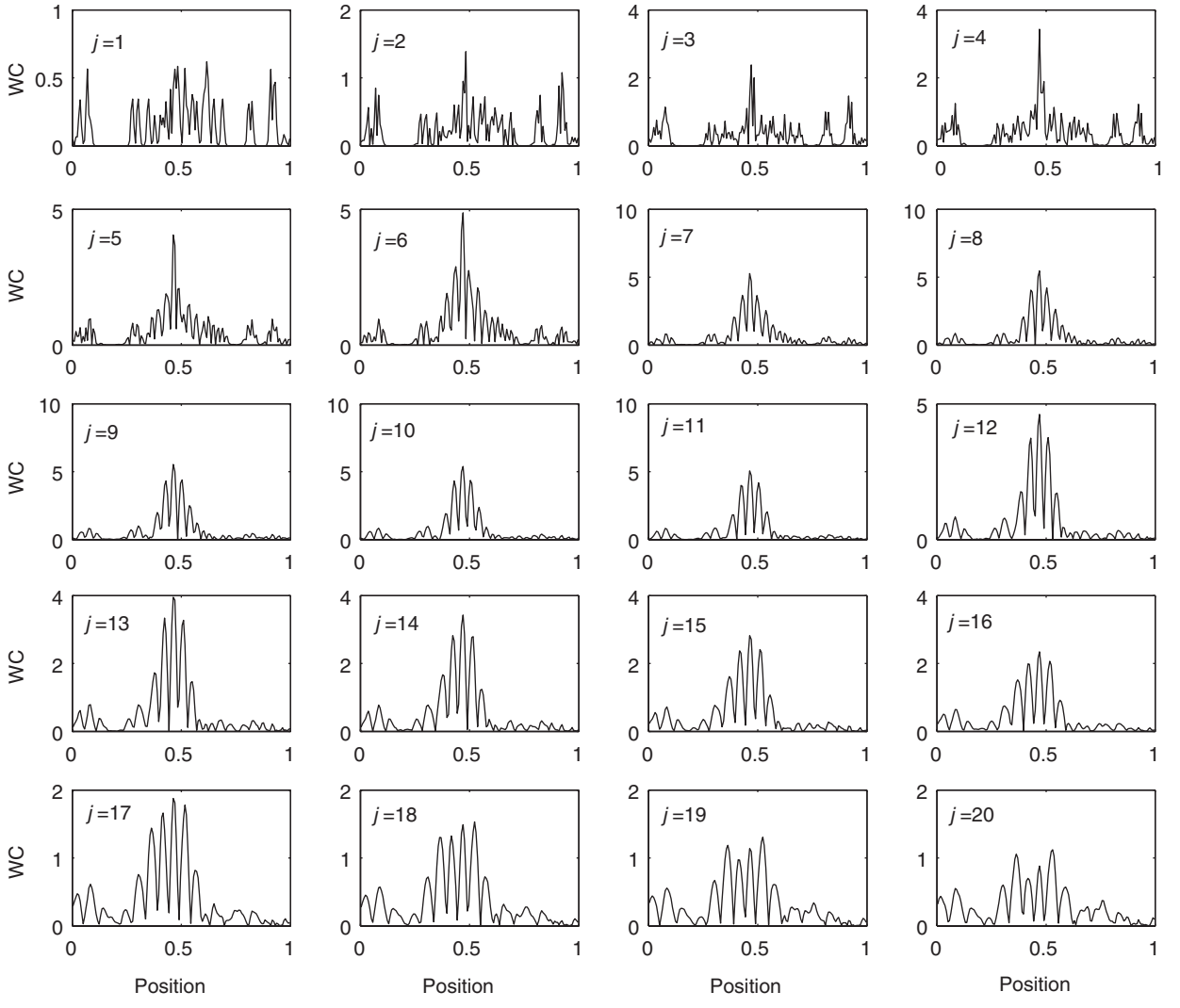

Fig. 2. $WC_1(x, j)$ for a damaged rod with Id = 0.1% for different scales. Defect at $x_d = 0.4767$ m.

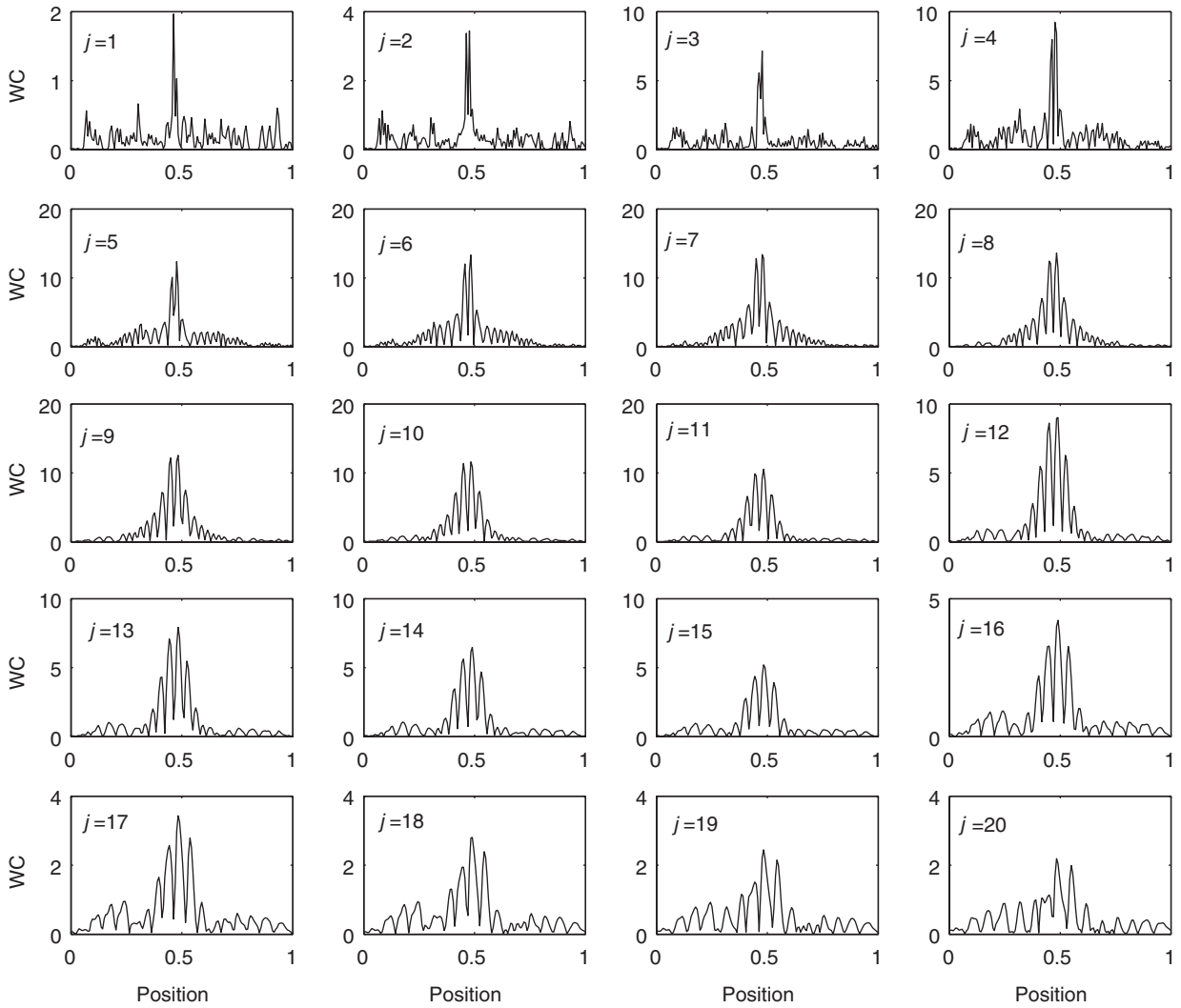

Fig. 3. $WC_1(x,j)$ for a damaged rod with Is = 0.1% for different scales. Defect at $x_d = 0.4767$ m.

Fig. 4 shows the signals $\xi_n^d(x)$ for $n = 1,\ldots,8$ with a defect at $x_d = 0.4767$ m and intensity Id = 0.01%. We can see no relevant change present at $x = x_d$ for any of the modes. Fig. 5 shows the plots of $WC_n(x,4)$ for $n = 1,\ldots,8$ and for a density type defect. For this intensity, for low modes, $n = 1$ and 2, the defect is indetectable. However, in general, the detection improves as the mode order increases. In Fig. 6, the maximum amplitude of the function $WC_n(x,4)$ is plotted for the eight vibration modes and the following set of intensities: Id = [0.01, 0.05, 0.1, 0.2, 0.4, 0.6, 0.8, 1]%. This characteristic can be used to evaluate the detection because the higher the value of $WC_n(x,j)$, the better the detection. The main observation is that for all the modes there is a clear linear correlation between the $WC_n(x,4)$ maximum value and the intensity of the defect, although the slope varies with the order of the vibration mode. This linear relation permits, not only the detection and localization of the defect; it also allows us to deduce its intensity (Level 3 in SHM).

A comparison between modes in Fig. 6 reveals that, in general, the well-known fact that higher-order modes are more suitable for the detection of defects, is essentially true (the higher the order, the higher the $WC_n(x,4)$ maximum value). However, modes 3 and 4 are interchanged, as are the modes 5 and 6. This observation leads us to conclude that another criterion besides mode order has to be considered. If we observe the waveform of the modes (see Fig. 4 and Table 1), we can deduce that at the defect position, x_d, the value of the displacement,

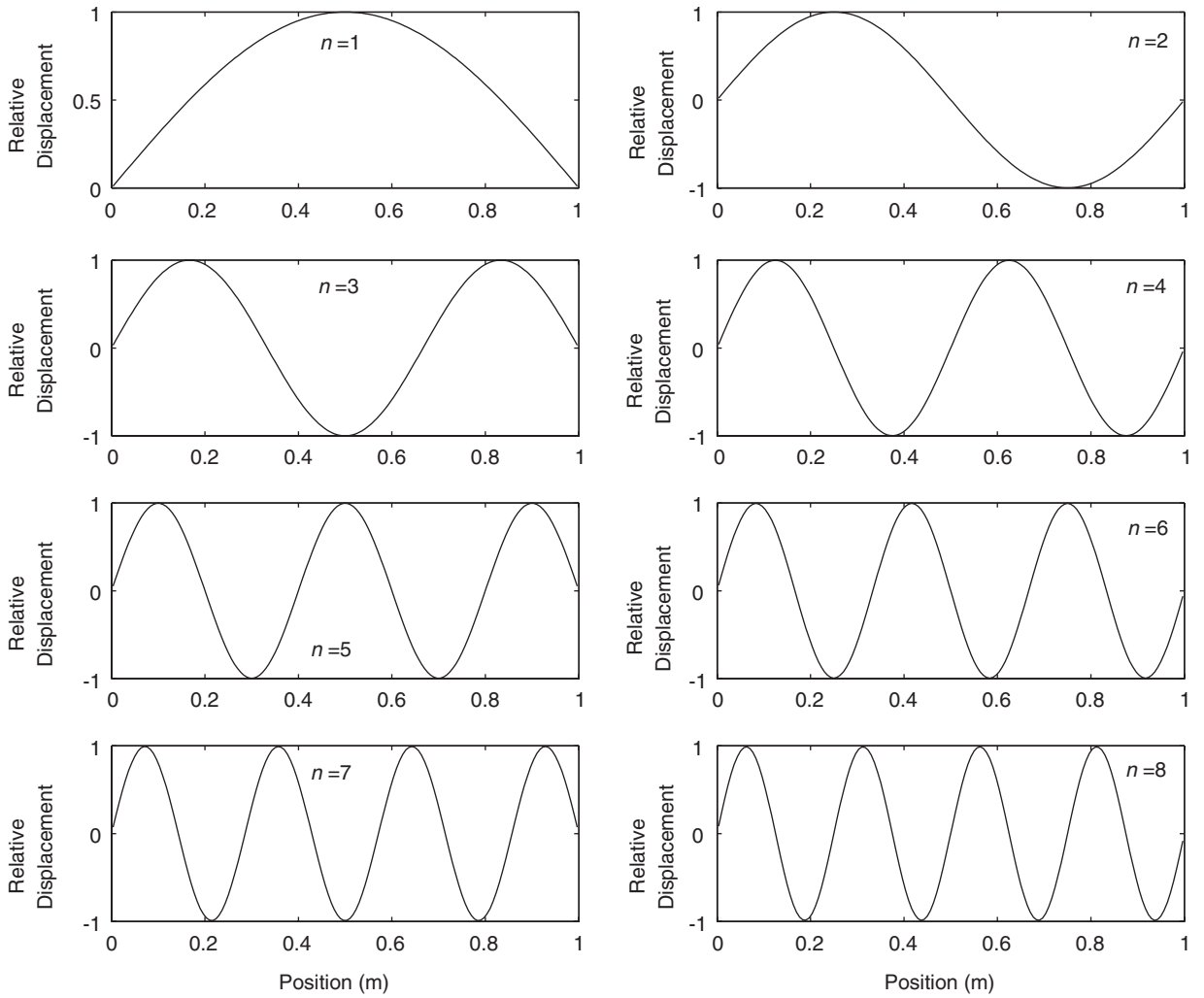

Fig. 4. First eight vibration modes of the rod.

$\xi_n^u(x_d)$, is different for each mode (each value of n). Thus, for modes in which the defect is located near a node (low absolute value of displacement), the value of the $WC_n(x,4)$ maximum will also be low, and thus, the detection quality will be worse. However, for modes in which the defect is located near an antinode (high absolute value of displacement), the value of the $WC_n(x,4)$ maximum will also be high, and detection will be better. This occurs, for example, for mode 3, $|\xi_3^u(x_d)| = 0.960$, and for mode 4, $|\xi_4^u(x_d)| = 0.368$, which justifies the aforementioned interchangeability between these two modes. In summary, two factors act at the same time, influencing the detection quality of each vibration mode: (1) the higher the mode order, the higher the detection quality; (2) the higher the value of the displacement at the point where the defect is located (in absolute value), the higher the detection quality. For this reason the increase or lack thereof of detectability with the mode number depends on the location of the defect, a feature that is not known a priori in realistic problems.

Figs. 7 and 8 show the same set of results for stiffness defects. It is clear that detection/location is possible for all the modes and intensities considered. The detection quality evaluated by means of the maximum of the $WC_n(x,4)$ parameter plotted in Fig. 8 shows an important difference between this type of defect and the density defect. By comparing Figs. 6 and 8, we can deduce that for the stiffness defect, although the detection quality tends to improve according to the mode order, the second factor acts differently. For example, mode 2

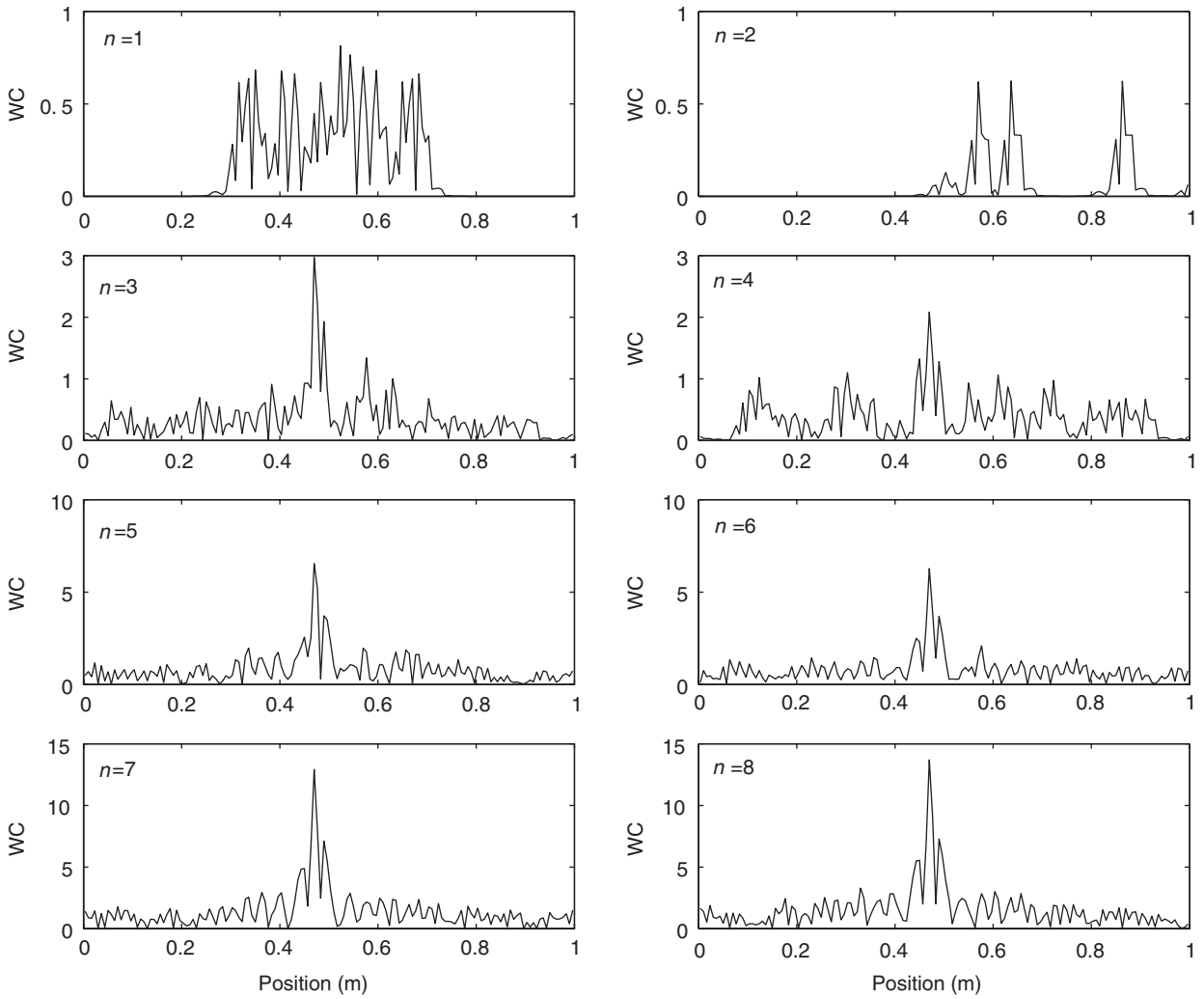

Fig. 5. $WC_n(x,2)$ for the first eight vibration modes. Damaged rod with Id = 0.1% and $x_d = 0.4767$ m.

is better than mode 3, mode 4 is better than mode 5, and mode 6 is better than mode 7. This behavior can be explained if we consider the shape of stress for the different modes, $|\sigma_n^u(x)|$, instead of the displacement. Using Eq. (2), the stress modes can be easily obtained from the displacement modes. Table 2 shows the value of $|\sigma_n^u(x_d)|$ (at the point in which the defect is located). We can see, for example, that $|\sigma_2^u(x_d)| > |\sigma_3^u(x_d)|$, $|\sigma_4^u(x_d)| > |\sigma_5^u(x_d)|$ and $|\sigma_6^u(x_d)| > |\sigma_7^u(x_d)|$, which justifies the behavior previously mentioned. Moreover, it can be seen that in this case mode 1 is very close to a node ($|\sigma_1^u(x_d)|$ is very close to zero), which is the reason why it is the poorest mode for detection of this kind and position of defect. Hence, for defects affecting stiffness, the second factor to keep in mind when choosing the best mode is the amplitude of the stress mode (in absolute value), rather than that of the displacement mode. To explain this fact, let us consider the Young modulus function along the rod

$$Y(x) = Y + Y_d\delta(x - x_d), \tag{7}$$

where δ is the Dirac function, which can be approximated by

$$\delta(x - x_d) \cong \exp\left(-\frac{(x - x_d)^2}{a^2}\right) \Big/ (a\pi^{1/2}) \quad a \to 0. \tag{8}$$

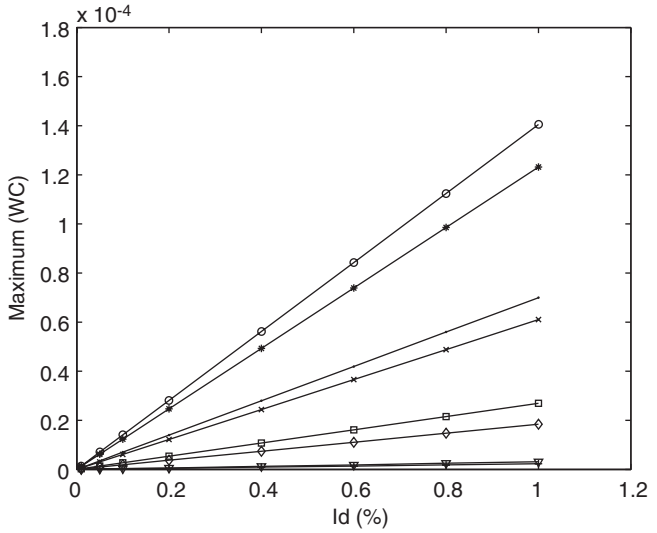

Fig. 6. Maximum of $WC_n(x,2)$ for different defect intensities (density type) and different modes. ∇: mode 1; $+$: mode 2; $\square$: mode 3; $\diamond$: mode 4; $\bullet$: mode 5; $\times$: mode 6; $*$: mode 7; $\circ$: mode 8.

Table 1
Displacement of the first eight vibration modes at the defect position ($\xi_n^u(x_d = 0.4767\,\mathrm{m})$)

Mode order	1	2	3	4	5	6	7	8
$\xi_n^u(x_d)$	0.996	0.187	−0.960	−0.368	0.891	0.536	−0.790	−0.685

Using this equation, together with Eqs. (1) and (2), the following relationship can be demonstrated

$$-Y(x)\,\frac{\partial^2\xi}{\partial x^2} - Y_d\,\frac{\partial\xi}{\partial x}\,e^{-(x-x_d)^2/a^2}\,\frac{2(x-x_d)}{a^3\pi^{1/2}} + \rho\,\frac{\partial^2\xi}{\partial t^2} = 0. \tag{9}$$

The second term in Eq. (9) is due to the defect. This term is proportional to the spatial derivative of displacement, i.e., to the stress. Thus, the higher the stress, the higher this term, and so higher the influence of the defect in the solution of the wave equation (Eq. (9)). This will occur whenever the defect is near a stress antinode, i.e. a displacement node.

4. Conclusions

Free longitudinal vibrations have been used for damage detection in rods via the CWT with the position as an independent variable. Local decreases in density and stiffness were considered, of very small size and intensity, to model the damage. We have shown it is possible to arrive at Level 3 of damage detection, even for local decreases in stiffness and density of up to 0.01%. The presence of a peak in the CWT allows localization of the defect, while the linear relationship between the amplitude of this peak and the intensity of the defect permits its quantification (Level 3).

The study of the influence of scale on the quality of defect detection leads us to the following conclusions:

- At lower scales the precision of localization improves because the peak width becomes lower.
- Highest peak amplitudes are reached at intermediate scales. Therefore, they stand out more clearly from the background noise, and so the detection, localization and quantification of the defect are all more efficient.

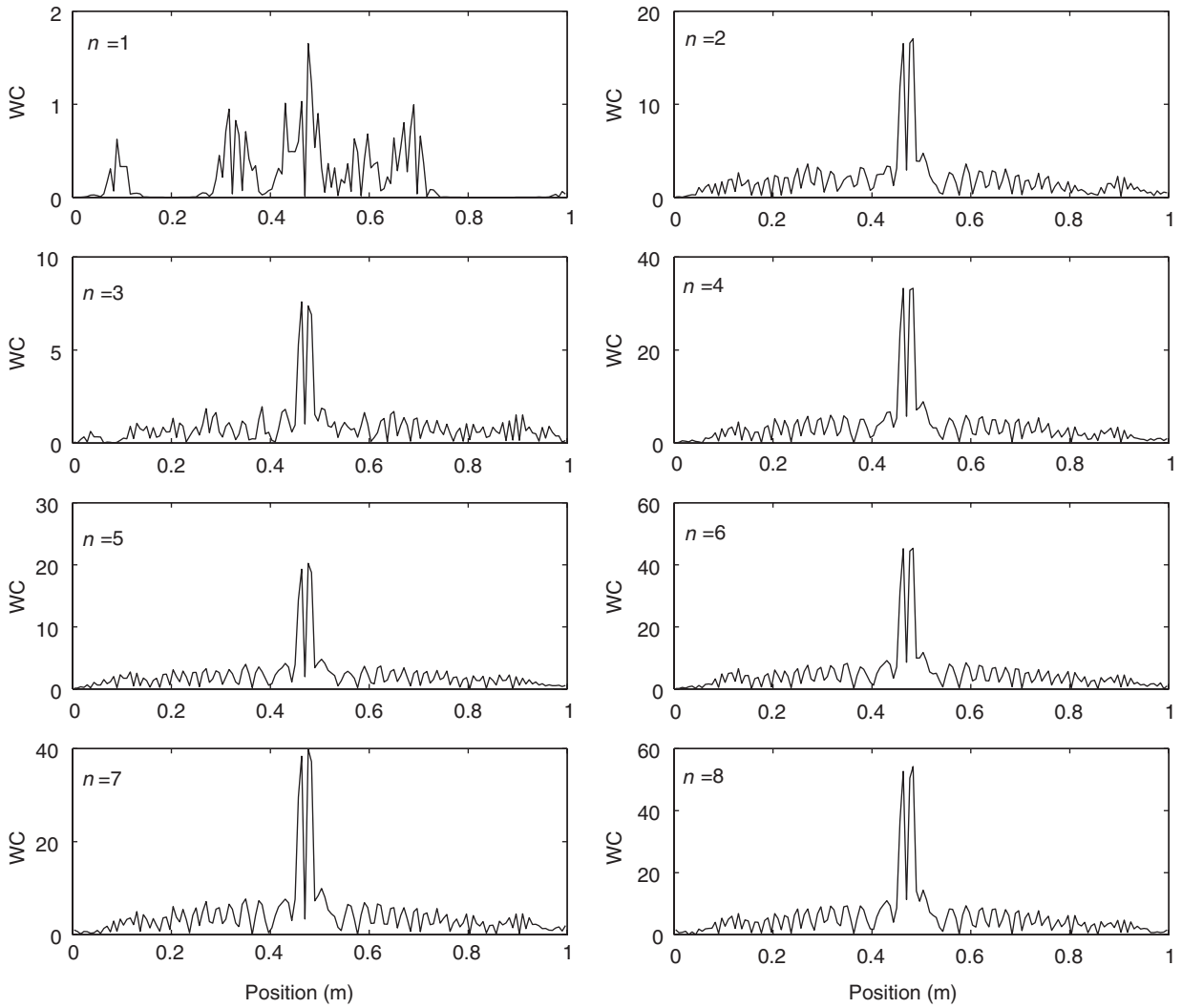

Fig. 7. $WC_n(x,2)$ for the first eight vibration modes. Damaged rod with Is = 0.1% and $x_d = 0.4767$ m.

The most relevant result of this study stems from the comparison of the different modes of vibration with regards to their capacity of detection of the defect. The first eight modes of vibration were considered; and the capacity of detection is shown to depend on the combination of two factors: the order of the used mode and the location of the defect.

For both types of defect, the higher the order of the mode, the better the detection. This is because the amplitude of the peaks in CWT is greater, and they can be discerned better against the background noise. This result can likewise be found in the literature, and it is physically logical, as the high frequency modes are affected more than the low frequency ones in the face of minor changes in the mechanical properties of the vibrating structure. Yet in practice, the high-order modes are more notably affected by the noise, which makes their use less than recommendable.

The second factor depends on the type of defect:

- If the defect is of the density type, the modes of displacement that have an antinode closer to the defect are the best for its detection.

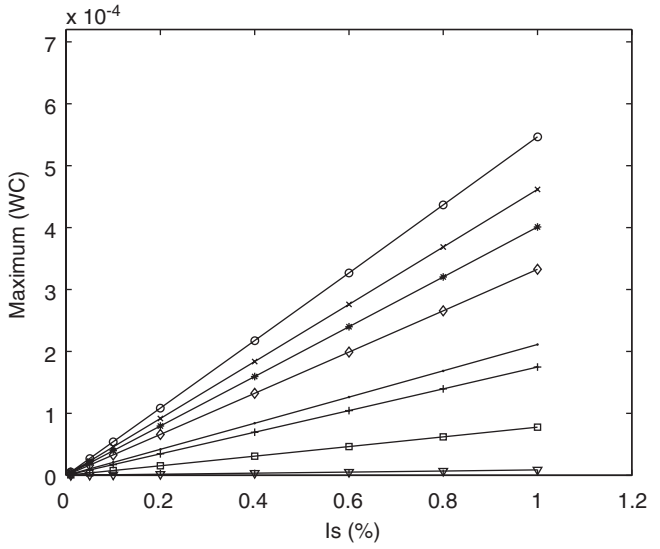

Fig. 8. Maximum of $WC_n(x,2)$ for different defect intensities (stiffness type) and different modes. ∇: mode 1; $+$: mode 2; $\square$: mode 3; $\diamond$: mode 4; $\bullet$: mode 5; $\times$: mode 6; $*$: mode 7; $\circ$: mode 8.

Table 2
Stress of the first eight vibration modes at the defect position ($\sigma_n^u(x_d = 0.4767\,\mathrm{m})$)

Mode order	1	2	3	4	5	6	7	8
$\sigma_n^u(x_d)$	0.094	−0.982	−0.279	0.930	0.454	−0.844	−0.613	0.729

- If the defect is of a stiffness type, the modes of displacement that have a node closer to the defect are the best for its detection. Note, that a node of the displacement corresponds with an antinode of the stress. This result is physically reasonable because, as demonstrated theoretically, a change of the Young modulus of the rod affects the stress modes more than it does the modes of displacement.

The position of the defect is not known in practice, for which reason we do not know which modes are best for detection, whether the odd or even ones. It is therefore adviseable to compare the result obtained with several consecutive modes of vibration, in view of the data presented here.

Acknowledgment

This study was funded in part by Spain's I + D National Plan DPI 2002-04472-C02-02 Project.

References

[1] E. Castro, M.T. García-Hernández, A. Gallego, Transversal waves in beams via the network simulation method, *Journal of Sound and Vibration* 283 (2005) 997–1013.
[2] F.K. Chang, Structural health monitoring 2000, *Proceedings of the Second International Workshop on SHM*, Stanford, 1999.
[3] C.P. Frietzen, G. Mengelkamp, A. Güemes, A CFRP plate with piezo-electric actuators and sensors as self-diagnosing intelligent structure, *Proceedings of the ISMA*, Leuven, Belgium, 2002.
[4] A. Rytter, Vibration Based Inspection of Civil Engineering Structures, PhD Thesis, Aalborg University, Denmark, 1993.
[5] K.M. Liew, Q. Wang, Application of wavelet theory for crack identification in structures, *Journal of Engineering Mechanics* 124 (1998) 152–157.
[6] A.V. Ovanesova, L.E. Suárez, Applications of wavelet transform to damage detection in frame structures, *Engineering Structures* 26 (2004) 39–49.

[7] H. Kim, H. Melhem, Damage detection of structures by wavelet analysis, *Engineering Structures* 26 (2004) 347–362.
[8] C.C. Chuang, L.W. Chen, Damage detection of a rectangular plate by spatial wavelet based approach, *Applied Acoustics* 65 (2004) 819–832.
[9] X. Deng, Q. Wang, Crack detection using spatial measurements and wavelet analysis, *International Journal of Fracture* 91 (1998) L23–L28.
[10] E. Douka, S. Loutridis, A. Trochidis, Crack identification in plates using wavelet analysis, *Journal of Sound and Vibration* 270 (2004) 279–295.
[11] W.J. Wang, Wavelet transform in vibration analysis for mechanical fault diagnosis, *Shock and Vibration* 3 (1996) 17–26.
[12] C.C. Chuang, L.W. Chen, Vibration damage detection of a Timoshenko beam by spatial wavelet based approach, *Applied Acoustics* 64 (2003) 1217–1240.
[13] J. Tian, Z. Li, X. Su, Crack detection in beams by wavelet analysis of transient flexural waves, *Journal of Sound and Vibration* 261 (2003) 715–727.
[14] C.J. Lu, Y.T. Hsu, Vibration analysis of an inhomogeneous string for damage detection by wavelet transform, *International Journal of Mechanical Sciences* 44 (2002) 745–754.
[15] Q. Wang, X. Deng, Damage detection with spatial wavelets, *International Journal of Solids and Structures* 36 (1999) 3443–3468.
[16] E. Castro, M.T. García-Hernández, A. Gallego, Network simulation method applied to vibration of rods, *Forum Acusticum*, Sevilla, September 2002.
[17] G. Rus, E. Castro, A. Gallego, J.L. Pérez-Aparicio, M.T. García-Hernández, Detection and location of damage in rods using wavelets of vibration simulated by the NSM and FEM, *II European Workshop on Structural Health Monitoring*, Munich, July 2004, pp. 465–476.
[18] K.F. Graff, *Wave Motion in Elastic Solids*, Dover Publications, New York, 1991.